Eur. Phys. J. C 16, 105–114 (2000)
Digital Object Identifier (DOI) 10.1007/s100520000412

THE EUROPEAN PHYSICAL JOURNAL C

$W\gamma$ and $Z\gamma$ production at hadron colliders

D. de Florian[1], A. Signer[2]

[1] Theoretical Physics, ETH Zürich, Switzerland
[2] Department of Physics, University of Durham, Durham DH1 3LE, UK

Received: 14 February 2000 / Published online: 18 May 2000 – © Springer-Verlag 2000

Abstract. We present a general purpose Monte Carlo program for the calculation of any infrared safe observable in $W\gamma$ and $Z\gamma$ production at hadron colliders at next-to-leading order in α_s. We treat the leptonic decays of the W and Z-boson in the narrow-width approximation, but retain all spin information via decay angle correlations. The effect of anomalous triple gauge boson couplings is investigated and we give the analytical expressions for the corresponding amplitudes. Furthermore, we propose a way to study the effect of anomalous couplings without introducing the ambiguity of form factors.

1 Introduction

The production of $W\gamma$ and $Z\gamma$ in hadronic collisions has been studied extensively since the Born cross sections have been computed [1,2]. In particular, these processes allow to study the triple gauge boson couplings $WW\gamma$, $ZZ\gamma$ and $Z\gamma\gamma$. The study of these couplings is mainly motivated by the hope that some new physics may modify them. If the new physics occurs at an energy scale well above that being probed experimentally, it is possible to integrate it out. The result is an effective theory which might result in non standard triple gauge boson couplings.

Both collaborations at the Tevatron have studied the production of $W\gamma$ [3] and $Z\gamma$ [4] pairs. The bounds on the anomalous couplings obtained at the Tevatron tend to be less constraining than those obtained at LEP [5]. However it has to be kept in mind that these analyses are complementary. At the hadron colliders a whole range in the center of mass energy is tested, whereas at LEP the center of mass energy is fixed by the collider. Furthermore, with Run II the expected number of events at the Tevatron increases substantially. Assuming a data sample of 2 fb^{-1}, more than 3000 $W\gamma \to \ell\nu\gamma$ events and 700 $Z\gamma \to \ell\ell\gamma$ events are expected for each experiment [6]. Of course, the expected number of events is even bigger for the LHC.

Anomalous triple gauge boson couplings lead to deviations from Standard Model predictions. Obviously, observables for which these deviations are enhanced offer better chances to find new physics or get tighter constraints on anomalous couplings. There are basically two classes of such observables. Either we consider observables which are strongly suppressed in the Standard Model or observables with large transverse momentum (or center of mass energy). In both cases, the inclusion of next-to-leading order (NLO) QCD corrections is mandatory.

A prominent example of an observable that is suppressed in the Standard Model is the so called radiation zero for $W\gamma$ production. At leading order (LO) there exist some kinematic configurations for which the amplitude vanishes [1]. This is manifest in some observables as a dip in the rapidity distributions. Since anomalous coupling contributions fill in the dips, there seemed to be excellent prospects to obtain accurate limits for them from experimental data. Unfortunately, next-to-leading order QCD corrections strongly affect the LO analysis. They have the same effect as the anomalous coupling contributions. The dips are filled in, making the extraction of anomalous couplings quite more difficult.

For processes with large transverse momentum or center of mass energy, the NLO corrections are particularly large. This is due to the fact that the cross sections in these cases get large contributions from gluon induced partonic subprocesses, which only enter in a next-to-leading order description of the cross section. Thus, even though the anomalous contributions are enhanced in these regions, a calculation at NLO in α_s is required to reliably exclude (or establish) physics beyond the Standard Model.

The relevance of NLO corrections was first shown for the production of real (spin-summed) W and Z bosons with Standard Model couplings and without considering lepton decays and spin correlations [7,8]. These calculations were later extended, in order to include the leptonic decays and anomalous couplings [9–11]. However, the full one-loop amplitudes including leptonic decays became available only very recently [12]. Therefore, [9–11] included decay correlations everywhere except for the finite part of the virtual contributions.

In this paper we present order α_s results for the production of $W\gamma$ and $Z\gamma$ in hadronic collisions, including the *full* leptonic correlations. We work in the narrow-width approximation, where only 'single-resonant' Feynman diagrams have to be considered. The simplicity of the helicity method allows to take into account anomalous couplings

as well and present for the first time analytical expressions for the corresponding amplitudes.

For the case of WW, ZZ and WZ production at hadron colliders, some results beyond the narrow-width approximation are known. The narrow-width approximation requires only the calculation of 'doubly-resonant' Feynman diagrams. However, for these processes, also the amplitudes including 'single-resonant' diagrams have been computed and implemented into a Monte Carlo program [13].

To perform the phase space integration we use the subtraction method discussed in [14]. This allows for a straightforward implementation of the one-loop $q\bar{q}' \to V\gamma \to \ell\ell'\gamma$ and bremsstrahlung $q\bar{q}' \to gV\gamma \to g\ell\ell'\gamma$ amplitudes, presented in [12] ($V \in \{Z, W\}$). The constructed Monte Carlo code allows the computation of any infrared-safe observable[1].

A brief overview of the calculation is given in Sect. 2, were we summarize the input parameters used and the cuts implemented to obtain our phenomenological results. In Sect. 3 we first present some benchmark cross section numbers for both $W\gamma$ and $Z\gamma$ production at the LHC and study the typical scale dependence of some observables at NLO in the Standard Model. Since many distributions have been studied in the past, we refrain from doing a detailed analysis. However, as soon as more precise data becomes available such an analysis can easily be done.

In Sect. 4 we concentrate on anomalous triple gauge boson couplings. We describe the parameterization of the triple gauge boson vertex in terms of anomalous coupling parameters and search for the kinematical region where its effect is amplified, namely at large transverse momentum for both photon and leptons. We also analyze the possibility of seeing the effect of approximate radiation zeros in the $W\gamma$ process, i.e. by looking for 'dips' in rapidity distributions. In order to avoid the arbitrariness introduced by form factors, we propose to analyze the anomalous couplings as a function of the squared partonic center of mass energy $\hat{s}$. This has been suggested previously for the $Z\gamma$ case [15], where such an analysis is straightforward. We extend this idea to the $W\gamma$ production. This case is more involved, since a complete reconstruction of $\hat{s}$ is impossible, due to the appearance of a non observed neutrino in the W decay. Particularly, we present an observable quantity which is highly correlated to $\hat{s}$ and, therefore, allows such an analysis even for $W\gamma$ production. Finally, in Sect. 5 we give our conclusions and in the appendix we present analytical expressions for the amplitudes relevant for the processes under consideration.

2 Formalism

The helicity amplitudes needed for the computation of the NLO corrections to $W\gamma$ and $Z\gamma$ production in the Standard Model were presented in [12]. The amplitudes relevant for the inclusion of anomalous couplings are presented in the appendix. In order to cancel analytically the soft and collinear singularities coming from the bremsstrahlung and one loop parts, we have used the version of the subtraction method presented in [14]. The amplitudes are therefore implemented into a numerical Monte Carlo style program, which allows to calculate any infrared-safe physical quantity with arbitrary cuts.

Obviously, the Monte Carlo program can be used for the Tevatron and the LHC. However, in this paper we will mainly concentrate on results for the LHC collider, which corresponds to pp scattering at $\sqrt{s} = 14$ TeV. Unless otherwise stated, the results are obtained using the following cuts: we make a transverse momentum cut of $p_T^\ell > 25$ GeV for the charged leptons and the rapidity is limited to $|\eta| < 2.4$ for all detected particles. The photon transverse momentum cut is $p_T^\gamma > 50(100)$ GeV for $W\gamma$ ($Z\gamma$) production. For the $W\gamma$ case we require a minimum missing transverse momentum carried by the neutrinos $p_T^{\text{miss}} > 50$ GeV. Additionally, charged leptons and the photons must be separated in the rapidity-azimuthal angle by $\Delta R_{\ell\gamma} = \sqrt{(\eta_\gamma - \eta_\ell)^2 + (\phi_\gamma - \phi_\ell)^2} > 0.7$. Moreover, since our calculation is done in the narrow-width approximation and, therefore, ignores the radiation of photons from the final state leptons, we apply an additional cut to suppress the contribution from the off-resonant diagrams. For that purpose, we require the transverse mass $M_T > 90$ GeV for $W\gamma$ production and the invariant mass of the $\ell\ell\gamma$ system $M_{\ell\ell\gamma} > 100$ GeV for the $Z\gamma$ case.

Finally, photons can also be significantly produced at LHC from the *fragmentation* of a final state parton[2]. Unfortunately, fragmentation functions of partons into photons are not very well determined and the NLO calculation for such a contribution is not available yet. In principle, a full NLO calculation should include it however, since only the sum of the 'direct' plus 'fragmentation' components is physically well defined at NLO (only in the sum all collinear singularities cancel out). In order to circumvent this problem, we include the LO component of the fragmentation part but using NLO fragmentation distributions, where we can factorize the final state $q\gamma$ collinear singularities. Since the 'fragmentation' component can be further suppressed implementing certain cuts (see below) the lack of its NLO calculation is not expected to affect the final result beyond the few percent level.

The fragmentation contribution constitutes a background to the search of anomalous couplings, since it does not involve any triple gauge boson coupling. Fortunately, there is a way to suppress its contribution by requiring the photons to be isolated from hadrons. In this paper we require the transverse hadronic momentum in a cone of size $R_0 = 0.7$ around the photon to be smaller than a small fraction of the transverse momentum of the photon

$$\sum_{\Delta R < R_0} p_T^{\text{had}} < 0.15\, p_T^\gamma \tag{1}$$

This completes the definition of our 'standard' cuts.

[1] The corresponding Fortran codes are available upon request

[2] This contribution is also known in the literature as 'bremsstrahlung'

When indicated, we also apply a jet-veto, which means that we reject any event where a jet of $p_T^{\rm jet} > 50$ GeV and $|\eta_{\rm jet}| < 2.5$ is observed.

In our results we do not include the branching ratios of the vector boson into leptons. They can be taken into account by simply multiplying our final results with the corresponding branching ratio. For both the LO and NLO results we use the latest (corrected) set of parton distributions of MRST(cor01) [16] and the two loop expression (with $n_f = 5$ for the typical scales of these processes) for the strong coupling constant with $\Lambda_{\overline{\rm MS}}(n_f = 4) = 300$ MeV which corresponds to $\alpha_s(M_Z) = 0.1175$. For the fragmentation component we use the fragmentation functions from [17].

Since we are particularly interested in the large p_T tail, which is more sensitive to the anomalous coupling contributions, we use (unless otherwise stated)

$$\mu^2 = \mu_{\rm st}^2 \equiv M_V^2 + \frac{1}{2}\left[(p_T^V)^2 + (p_T^\gamma)^2\right] \qquad (2)$$

as the 'standard' scale for both the factorization and renormalization scales.

Contributions from b and t quark initial states have been neglected and, consistently, the following values have been used for the Cabibbo-Kobayashi-Maskawa (CKM) matrix elements in the case of $W\gamma$ production: $|V_{ud}| = |V_{cs}| = 0.975$ and $|V_{us}| = |V_{cd}| = 0.222$.

The masses of the vector bosons have been set to $M_Z = 91.187$ GeV and $M_W = 80.41$ GeV. We do not include any QED or electroweak corrections but choose the coupling constants α and $\sin^2\theta_W$ in the spirit of the 'improved Born approximation' [18,19], with $\sin^2\theta_W = 0.230$. Notice that the observable is order α^2; within the same spirit we use the running $\alpha = \alpha(M_Z) = 1/128$ for the coupling between the vector boson and the quarks (to effectively take into account the EW corrections) whereas we keep $\alpha = 1/137$ for the photon coupling. It is worth noticing that this modification results in a 7% change in the normalization of the cross section with respect to the standard approach of using both running coupling constants.

3 Standard results

We begin the presentation of our results with some total cross section numbers in Table 1, which can be useful for future checks and for an estimate of the number of events to be observed at the LHC. The first three results were obtained by imposing only the cut on the transverse momentum of the photon, i.e. $p_T^\gamma > 50(100)$ GeV for $W\gamma$ ($Z\gamma$) production. Apparently, the NLO corrections as well as the fragmentation contribution are very large. As discussed above, the relative importance of the fragmentation contribution can be reduced substantially by applying the isolation cut prescription. This can be seen from the results for the total cross section obtained after the implementation of our standard cuts, which are also presented in Table 1. Unfortunately, most of the previous publications on the subject [8–11] do not present cross sections numbers. Nevertheless, we have compared many of the plots shown in [8–11], specially for the case of real (spin-summed) $W/Z\gamma$ production [8] (which is not affected by lepton correlations). Within the precision that can be reached in such a comparison, we found good agreement.

Table 1. Cross sections in pb for pp collisions at $\sqrt{s} = 14$ TeV for $\mu = \mu_{\rm st}$. The statistical errors are ± 1 within the last digit. LO* corresponds to the direct component only

σ	LO*	Frag.	NLO
$W^+\gamma$ ($p_T^\gamma > 50$ GeV)	4.79	3.02	13.89
$W^-\gamma$ ($p_T^\gamma > 50$ GeV)	3.08	3.55	10.15
$Z\gamma$ ($p_T^\gamma > 100$ GeV)	1.29	0.412	2.37
$W^+\gamma$ (std. cuts)	0.436	0.094	1.71
$W^-\gamma$ (std. cuts)	0.310	0.095	1.20
$Z\gamma$ (std. cuts)	0.524	0.041	0.877

In what follows we will estimate the theoretical uncertainty of our results by analyzing the variation of various distributions when changing the scale μ by a factor of two in both directions $1/2\mu_{\rm st} \le \mu \le 2\mu_{\rm st}$. Since many observables already have been studied in the past [8–11] and in order to avoid the proliferation of plots, we refrain from presenting a detailed analysis here. We simply concentrate on a couple of typical examples in order to give a general picture and illustrate the importance of NLO corrections in both $W\gamma$ and $Z\gamma$ production.

In Fig. 1 we show the scale dependence of the p_T distribution of the photon in $W^+\gamma$ production with the standard cuts applied (upper curves) and also with the additional requirement of a jet-veto (lower curves). As can be observed, the scale dependence is still large ($\pm 10\%$) as long as only the standard cuts are applied. However, it is considerably reduced when the jet-veto is applied. The situation is similar to what has been observed in the case of WW production [20] and is caused by the suppression of the contribution from the qg initial state appearing for the first time at NLO. Since this initial state dominates the cross section, the NLO result behaves, regarding the scale dependence, effectively like a LO one.

In the inset plot we present the ratio between the NLO and LO results (with the standard scale), which remains larger than 3 and increases with the photon transverse momentum. This clearly shows that the LO calculation is not even sufficient for an understanding of the shape of the distribution, since the NLO effect goes beyond a simple change in the normalization. As is well known [8], the relevance of the NLO corrections for this process is mainly due to the breaking of the radiation zero appearing at LO and to the large qg initial state parton luminosity at the LHC. We also show the ratio of the NLO jet-veto and the LO result. As expected, this ratio is closer to 1, again due to the fact that most of the contributions coming from the new subprocesses appearing at NLO are suppressed by the jet-veto.

It is worth mentioning that the scale dependence of the LO result turns out to be very small. This is an arti-

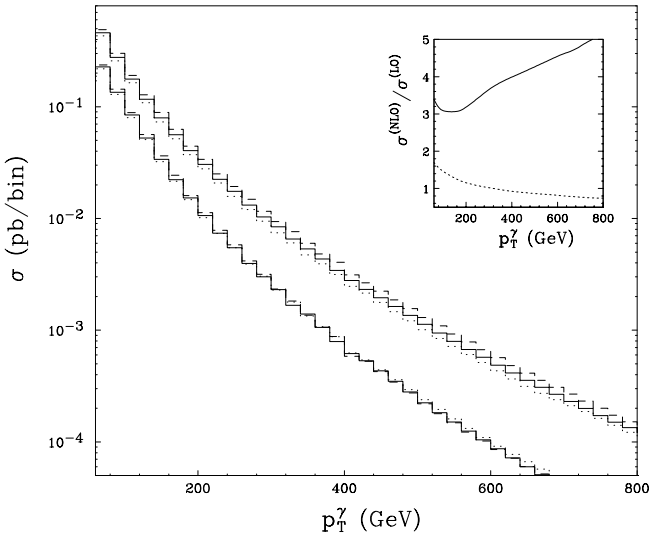

Fig. 1. Scale dependence of $\sigma^{(NLO)}$ without (upper curves) and with (lower curves) jet-veto. The scale has been varied according to $\frac{\mu_{\rm st}}{2}$(dashes) $< \mu <$ $2\mu_{\rm st}$(dots). The inset plot shows the ratio $\sigma^{(NLO)}/\sigma^{(LO)}$, again without (solid) and with (dots) jet-veto

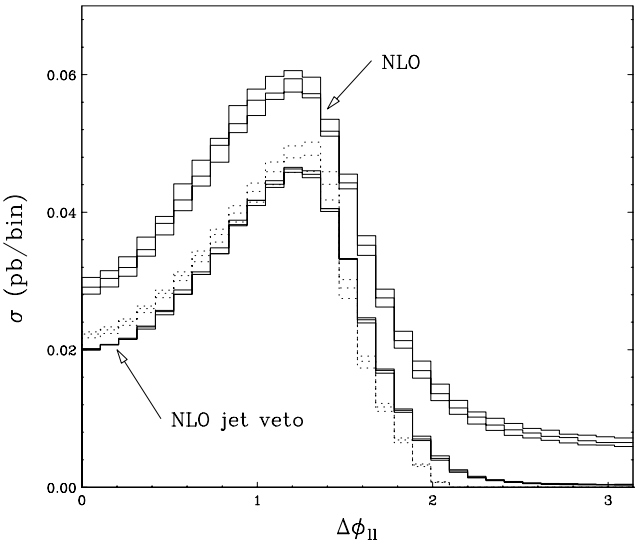

Fig. 2. Scale dependence of $\sigma^{(NLO)}$ without jet-veto (upper solid curves), $\sigma^{(NLO)}$ with jet-veto (lower solid curves) and $\sigma^{(LO)}$ (dotted curves). The scale has been varied according to $\frac{\mu_{\rm st}}{2} < \mu < 2\mu_{\rm st}$

ficial effect and illustrates that a small scale dependence is by no means a guaranty for small NLO corrections. In fact, there is no renormalization scale dependence at all at LO. The only scale dependence comes from the factorization scale dependence of the parton distribution functions. Furthermore, we would like to mention that the situation concerning the scale dependence is slightly more favorable at the Tevatron. This is simply due to the fact that the gluon initiated process is less important.

In Fig. 2 we study the lepton correlation in the azimuthal angle for $Z\gamma$ production, $\Delta\phi_{\ell\ell} = |\phi_{\ell^-} - \phi_{\ell^+}|$. Notice that this observable can be studied at NLO since we take fully into account the spin correlations between the leptons in our implementation of the one-loop corrections. The NLO corrections are rather sizeable and increase the cross section by 50% for small $\Delta\phi_{\ell\ell}$. The region $\Delta\phi_{\ell\ell} > 2$ (with our standard cuts) is kinematically forbidden unless a jet with a high transverse momentum is produced. Therefore, the cross section vanishes at LO and it is strongly suppressed for the NLO calculation with jet-veto. In this region, the full NLO calculation is effectively only a LO calculation and its scale dependence becomes larger, as expected.

Because there is no radiation zero appearing at LO for $Z\gamma$ production, the NLO corrections are under better control in the kinematical region where the LO cross section does not vanish. Nevertheless, for large transverse momentum, the process with a qg initial state again dominates the NLO contribution and the corrections increase considerably [10].

Finally we mention that we also considered a more stringent photon isolation prescription, introduced by Frixione [21]. This prescription completely eliminates the fragmentation contribution. We have checked that the main features of all studied distributions remain unchanged when it is imposed.

4 Sensitivity to anomalous couplings

The study of triple gauge boson couplings is motivated by the hope that some physics beyond the Standard Model leads to a modification of these couplings which eventually could be detected. In order to quantify the effects of the new physics an effective Lagrangian is introduced which in principle contains all Lorentz invariant terms. The prefactor of these operators are the anomalous couplings. A general approach is impractical, since it would lead to a proliferation of new couplings. Therefore, some additional constraints have to be imposed.

The usual choice for $W\gamma$ production is to insist on electromagnetic gauge invariance and on C and P invariance. Also, only operators of dimension six or less are considered. This leads to a momentum-space vertex $W^-_\alpha(q)W^+_\beta(\bar{q})\gamma_\mu(p)$ (where all momenta are outgoing $p + q + \bar{q} = 0$) which can be written as [22,20]

$$\begin{aligned}
&\Gamma^{\alpha\beta\mu}_{WW\gamma}(q,\bar{q},p)\\
&= \bar{q}^\alpha g^{\beta\mu}\left(2 + \Delta\kappa^\gamma + \lambda^\gamma\frac{q^2}{M_W^2}\right)\\
&\quad -q^\beta g^{\alpha\mu}\left(2 + \Delta\kappa^\gamma + \lambda^\gamma\frac{\bar{q}^2}{M_W^2}\right)\\
&\quad +(\bar{q}^\mu - q^\mu)\left[-g^{\alpha\beta}\left(1 + \frac{1}{2}p^2\frac{\lambda^\gamma}{M_W^2}\right) + \frac{\lambda^\gamma}{M_W^2}p^\alpha p^\beta\right], \quad (3)
\end{aligned}$$

where the overall coupling has been chosen to be $-|e|$. Note that in the Feynman rule for this vertex there is also

a factor i that is conventionally not included in $\Gamma^{\alpha\beta\mu}$. In the Standard Model we have $\Delta\kappa^\gamma = \lambda^\gamma = 0$.

For $Z\gamma$ production, we consider operators up to dimension 8 (all of them C odd) resulting in $ZZ\gamma$ and $Z\gamma\gamma$ couplings. The non-standard $Z_\alpha(q_1)\gamma_\beta(q_2)Z_\mu(p)$ momentum-space vertex is given by [15]

$$\Gamma^{\alpha\beta\mu}_{Z\gamma Z}(q_1,q_2,p) = \frac{i(p^2-q_1^2)}{M_Z^2}\Bigg(h_1^Z\left(q_2^\mu g^{\alpha\beta} - q_2^\alpha g^{\mu\beta}\right) + \frac{h_2^Z}{M_Z^2}p^\alpha\left(P\cdot q_2\; g^{\mu\beta} - q_2^\mu p^\beta\right) - h_3^Z\varepsilon^{\mu\alpha\beta\nu}q_{2\,\nu} - \frac{h_4^Z}{M_Z^2}\varepsilon^{\mu\beta\nu\sigma}p^\alpha p_\nu q_{2\,\sigma}\Bigg) \quad (4)$$

where the overall coupling has been chosen to be $|e|$ (and $\epsilon^{0123} = +1$). This vertex is absent altogether in the Standard Model. The non-standard $Z_\alpha(q_1)\gamma_\beta(q_2)\gamma_\mu(p)$ momentum-space vertex can be obtained from (4) by setting $q_1^2 \to 0$ and replacing $h_i^Z \to h_i^\gamma$. Notice that the vertex differs from the one implemented in [11] by an overall factor i, which ensures the hermiticity of the corresponding effective Lagrangian[3] [15]. Furthermore, the i factor modifies the interference pattern of anomalous coupling and Standard Model amplitudes: CP-violating $h_{1,2}$ contributions do not interfere with the Standard Model ones, whereas the CP-conserving $h_{3,4}$ do [15]. Therefore, with the corrected vertex, there are contributions linear in $h_{3,4}$ and the cross section is generally not invariant anymore under a change of sign of $h_{3,4}$. This must be considered in a future precise analysis of anomalous couplings from experimental data since the limits for $h_{3,4}$ will not be symmetric at variance with present analyses.

The anomalous couplings spoil the gauge cancellation in the high energy limit and, therefore, will lead to violation of unitarity for increasing partonic center of mass energy $\sqrt{\hat{s}}$. Usually, in an analysis of anomalous couplings from experimental data in hadronic collisions this problem is circumvented by supplementing the anomalous couplings, $\alpha_{\rm AC}$, with form factors. A common choice for the form factor is

$$\alpha_{\rm AC} \to \frac{\alpha_{\rm AC}}{(1+\frac{\hat{s}}{\Lambda^2})^n} \quad (5)$$

where n has to be large enough to ensure unitarity and Λ is interpreted as the scale for new physics. Obviously, this procedure is rather ad hoc and introduces some arbitrariness [23]. Also, it is not really consistent with the effective theory approach. Increasing anomalous contributions would require the inclusion of even higher dimensional operators. At the end of this section section we will address the question on how to avoid this arbitrariness in an analysis of anomalous couplings at hadron colliders.

Anomalous couplings mainly affect the events with large $\hat{s}$ or large p_T. Since the total cross section is dominated by low p_T events this is not a good observable to get tight constraints on anomalous couplings. A more promising possibility is to consider a double binned cross section. We therefore consider the total cross section binned in p_T^ℓ and p_T^γ for the process $pp \to W^+\gamma \to \ell^+\nu\gamma$ at the LHC. In Fig. 3 we show the ratio of $\sigma_{\rm AC}$ over $\sigma_{\rm SM}$ where $\sigma_{\rm SM}$ is the Standard Model cross section and $\sigma_{\rm AC}$ is the cross section obtained with $\Delta\kappa = 0.08$ and $\lambda = 0.02$ (both within the present experimental limits from LEP [5] and Tevatron [24]) and a form factor as defined in (5) with $n = 2$ and $\Lambda = 2$ TeV. As expected, the ratio is large for the high p_T bins, whereas it is very close to one for the low p_T bins. We checked that the uncertainty coming from the scale variation is much smaller than the effect of the anomalous couplings for the high p_T bins.

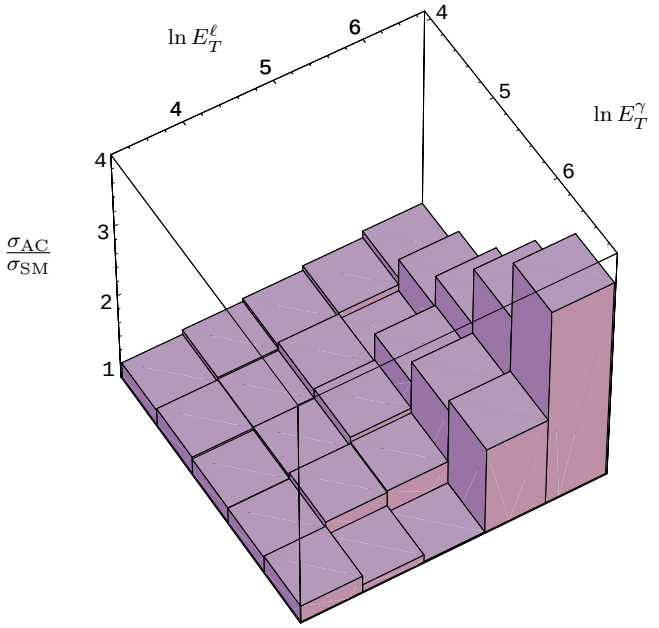

Fig. 3. Ratio of $\sigma_{\rm AC}$ and $\sigma_{\rm SM}$ at NLO for $\mu = \mu_{\rm st}$. The anomalous couplings in $\sigma_{\rm AC}$ have been chosen as $\Delta\kappa^\gamma = 0.08, \lambda^\gamma = 0.02$ and a form factor defined in (5) with $n = 2$ and $\Lambda = 2$ TeV has been used

Another possibility to get a large effect due to anomalous couplings is to consider the approximate radiation zeros present in the $W\gamma$ process [1]. At tree-level in the Standard Model, the $\Delta\eta_{W\gamma} \equiv \eta_W - \eta_\gamma$ distribution has a radiation zero. This dip is filled by next-to-leading order corrections and anomalous effects. In order to get an observable quantity, we do not consider $\Delta\eta_{W\gamma}$ but rather $\Delta\eta_{\gamma\ell}$ [25]. This will wash out the dip as the rapidity of the lepton is not equal to the rapidity of the W. However, requiring the energy (or the transverse momentum) of the lepton to be large enough forces the lepton to follow closely the W direction. Also, applying a jet-veto reduces the effects of the next-to-leading order corrections. Thus, for larger p_T^ℓ even the next-to-leading order $\Delta\eta_{\gamma\ell}$ distribution shows a clear dip in the Standard Model. This is illustrated in Fig. 4, where we show the $\Delta\eta_{\gamma\ell}$ distribution for the standard cuts and the additional cuts $p_T^\ell > 100$ GeV and $p_T^\ell > 200$ GeV respectively. In all figures we ap-

[3] There is also a sign difference in the $h_{3,4}$ contributions coming from the different definition of ϵ^{0123} in [11]

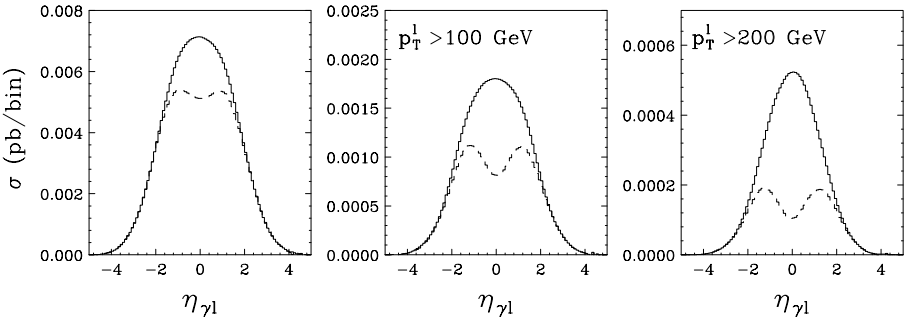

Fig. 4. $\Delta\eta_{\gamma\ell}$ distribution at NLO without (dashed curves) and with anomalous couplings $\Delta\kappa^\gamma = 0.08, \lambda^\gamma = 0.02$ (solid curves). In the first plot we applied only standard cuts and the jet-veto, in the second plot there is an additional cut $p_T^\ell > 100$ GeV, and in the third plot $p_T^\ell > 200$ GeV

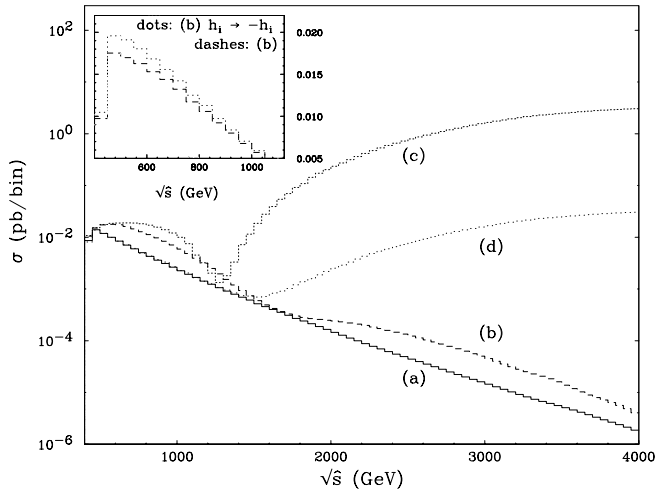

Fig. 5. Cross section at NLO for $\mu = \mu_{\rm st}$ with standard cuts and $p_T^\gamma > 200$ GeV and $p_T^Z > 200$ GeV. (a) no anomalous couplings; (b) $h_3^\gamma = h_3^Z = 0.01,\ h_4^\gamma = h_4^Z = 10^{-4}$ and the usual dipole form factor with $\Lambda = 2$ TeV; (c) $h_3^\gamma = h_3^Z = 0.01,\ h_4^\gamma = h_4^Z = 10^{-4}$ and no form factor; (d) $h_3^\gamma = h_3^Z = 0.001,\ h_4^\gamma = h_4^Z = 10^{-5}$ and no form factor. The inset plot shows again (b) and (b) with the opposite sign in the anomalous couplings

ply our jet-veto. Also shown are the three distributions with anomalous couplings, which are chosen as for Fig. 3. Clearly, the effect is dramatic for high energy leptons but of course, the disadvantage of applying such a cut is a big loss in statistics.

We now turn to the question whether it is possible to avoid using form factors in the analysis of anomalous couplings at hadron colliders. This would bring these analyses more into line with those at e^+e^- colliders. In order to do so one should analyze the data at fixed values of $\hat{s}$, as it is done at LEP. This results in limits for the anomalous parameters which are a function of $\hat{s}$.

Obviously, it is possible to do such analysis for the production of $Z\gamma$ when both leptons are detected. Since the center of mass partonic energy can be reconstructed from the kinematics of the final state particles[4] the cross section can be measured for different bins of fixed $\hat{s}$ [15]. As an example, we show in Fig. 5 the cross section as a function of $\hat{s}$. In order to enhance the effect of the anomalous couplings we do not only apply our standard cuts but we also require $p_T^\gamma > 200$ GeV and $p_T^Z > 200$ GeV. We show four curves: the curve (a) is the Standard Model result; curve (b) includes anomalous couplings in the standard way, that is with a form factor as defined in (5) with $n = 3$ ($n = 4$) for $h_3^V (h_4^V)$ and $\Lambda = 2$ TeV and we have set $h_3^\gamma = h_3^Z = 0.01,\ h_4^\gamma = h_4^Z = 10^{-4}$; curve (c) uses the same values for $h_i^{Z/\gamma}$ but does not include any form factor; finally curve (d) does also not include any form factors but the anomalous couplings are smaller $h_3^\gamma = h_3^Z = 0.001,\ h_4^\gamma = h_4^Z = 10^{-5}$. For all of them we set $h_1^V = h_2^V = 0$. Of course, for large $\hat{s}$ the effects are much more dramatic if the form factor is omitted and at some point the corresponding curves would violate unitarity. This simply reflects the breakdown of the effective theory approach in this region. The idea behind Fig. 5 is that such an analysis can be done for suitably defined bins in $\hat{s}$. As a result, for each bin, i.e. each value of $\hat{s}$ a bound on the anomalous couplings can be obtained.

In the inset plot we present again curve (b) and the one corresponding to the parameters of (b) but with the opposite sign for values of the anomalous couplings $h_3^\gamma = h_3^Z = -0.01,\ h_4^\gamma = h_4^Z = -10^{-4}$. From there the effect of the interference between AC and SM results can be observed, i.e. the contribution of linear terms in h_3^V and h_4^V appearing in the squared amplitudes due to the correct treatment of the i factor in the $Z\gamma V$ vertex [15]. For this particular configuration, the interference effects are mostly relevant at $\sqrt{\hat{s}} < 1$ TeV and modify the cross section by more than 10%. Clearly, they must be taken into account in a precise extraction of anomalous couplings from future experimental data. Results for $h_{1,2}^V$ couplings are similar to those obtained for the same values of $h_{3,4}^V$. The only difference comes from the fact that the CP-violating couplings do not interfere with the SM. For a configuration like (b) with $h_1^\gamma = h_1^Z = 0.01,\ h_2^\gamma = h_2^Z = 10^{-4}$, the cross section is given by the average of both curves in the inset plot of Fig. 5.

The situation is more complicated for $W\gamma$ production since the neutrino is not observed. Nevertheless, by identifying the transverse momentum of the neutrino with the missing transverse momentum, and assuming the W boson to be on shell, it is possible to reconstruct the neutrino kinematics (particularly the longitudinal momentum) with a twofold ambiguity. In the case of the Tevatron, since it is a $p\bar{p}$ collider, it is possible to choose the

[4] To simplify the discussion we assume that *all* final state particles are detected, including the jets.

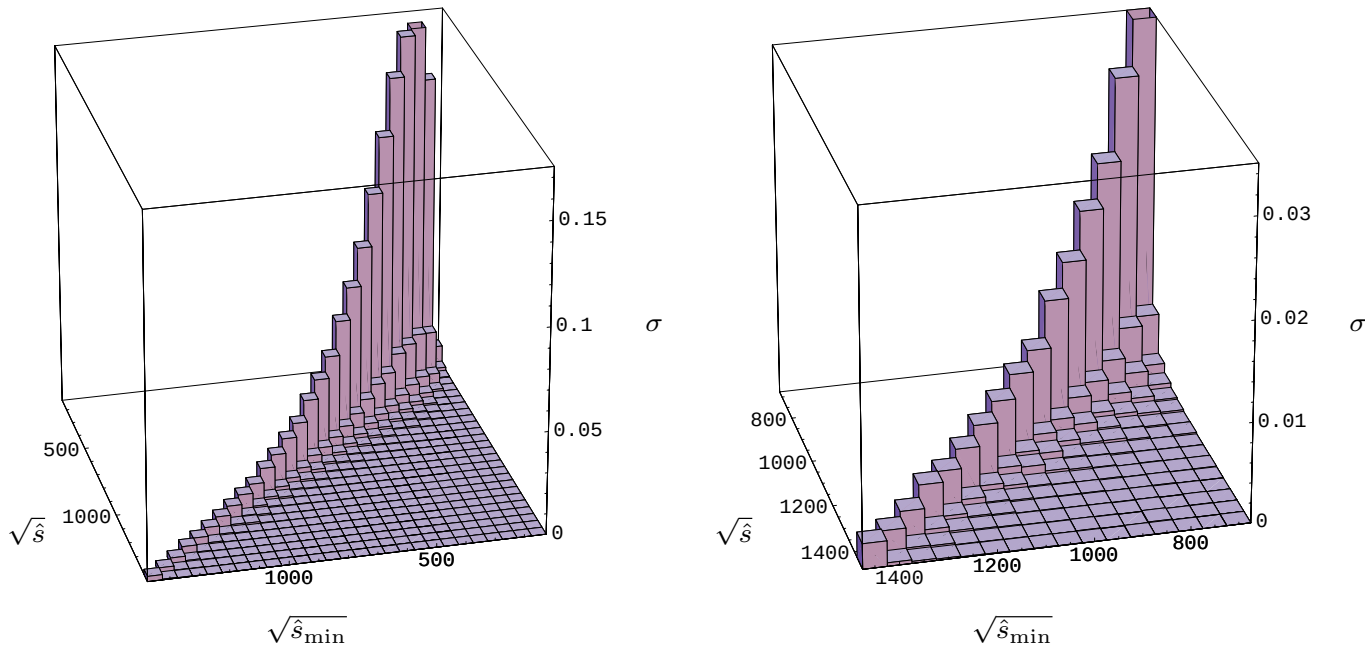

Fig. 6. The cross section for $W^+\gamma$ production(in pb/bin) as as function of $\sqrt{\hat{s}}$ and $\sqrt{\hat{s}_{\min}}$ (in GeV) in order to illustrate the steep fall of σ for increasing $|\sqrt{\hat{s}} - \sqrt{\hat{s}_{\min}}|$. The left plot shows the full range of $\sqrt{\hat{s}}$ whereas the right plot concentrates on the particularly interesting large $\sqrt{\hat{s}}$ region

'correct' neutrino kinematics 73% of the times by selecting the maximum (minimum) of the two reconstructed values for the longitudinal momentum of the neutrino for $W^+\gamma$ ($W^-\gamma$) [26].

This is not true at the LHC, where due to the symmetry of the colliding beams both reconstructed kinematics have equal chances to be correct. Fortunately, in the case of anomalous couplings, we are interested in a efficient way to reconstruct the $\hat{s}$ rather than the full kinematics. Again there are two possible values of $\hat{s}$. It turns out that there is a simple method to choose the 'correct' one 66% of the times at the LHC (73% of the times at Tevatron) by selecting the minimum $\hat{s}_{\min}$ of the two reconstructed values. This applies to both $W^+\gamma$ and $W^-\gamma$ production. Furthermore, we checked that the selected value $\hat{s}_{\min}$ differs in almost 90% of the events by less than 10% from the exact value $\hat{s}$. This is likely to be precise enough, since the data will be collected in sizeable bins of $\hat{s}$ and the anomalous parameters are not expected to change very rapidly as a function of the energy. To quantify the advantage of the method, we show in Figs. 6 and 7 the correlations of $\sqrt{\hat{s}_{\min}}$ with $\sqrt{\hat{s}}$. The cross section drops very rapidly for increasing $\sqrt{\hat{s}} - \sqrt{\hat{s}_{\min}}$. This correlation also holds in the particularly interesting large $\sqrt{\hat{s}}$ region and also for the anomalous contribution. To investigate the latter point, we show in Fig. 7 the correlation for (already experimentally ruled out) huge values of $\Delta\kappa = 0.8$ and $\lambda = 0.2$. For this figure we still use an ordinary form factor but in order to increase the anomalous contribution further we set $\Lambda = 1$ TeV.

Finally, in Fig. 8 we show the same correlation for $W\gamma$ production at the Tevatron (Run II), which corresponds to $p\bar{p}$ scattering at $\sqrt{s} = 2$ TeV. We impose the same kinematical cuts as for the LHC, with the following exceptions: for the transverse momentum of the photon we require $p_T^\gamma > 10$ GeV and the rapidities of the observed lepton has to be in the range $|\eta| < 1.5$ (instead of 2.4). As for the LHC, there is a strong correlation between the 'true' center of mass energy $\sqrt{\hat{s}}$ and the 'reconstructed' one $\sqrt{\hat{s}_{\min}}$. Again, this correlation also holds in the large $\sqrt{\hat{s}}$ region. In Fig. 8 no anomalous couplings are included, but we have checked that also for the Tevatron the inclusion of large anomalous couplings does not spoil the correlations.

As a result of these investigations we conclude that even in the case of $W\gamma$ production reliable bounds for anomalous couplings as a function of $\hat{s}$ can be obtained. To this end one merely has to do an analysis as in the $Z\gamma$ case but with $\hat{s}_{\min}$ replacing $\hat{s}$. This has the advantage that the anomalous effects can be quantized without introducing the ambiguity of form factors. Such a procedure would certainly facilitate a comparison of various bounds from different experiments. Finally, we note that in principle any quantity which has a very strong correlation with $\hat{s}$ can be used. However, we could not find any better candidate than $\hat{s}_{\min}$. In particular, the correlations of $\hat{s}$ with the cluster mass and transverse mass respectively is not quite as strong [27].

5 Conclusions

In this work, we have presented a general purpose Monte Carlo program for the calculation of any infrared safe observable in $W\gamma$ and $Z\gamma$ production at hadron colliders at

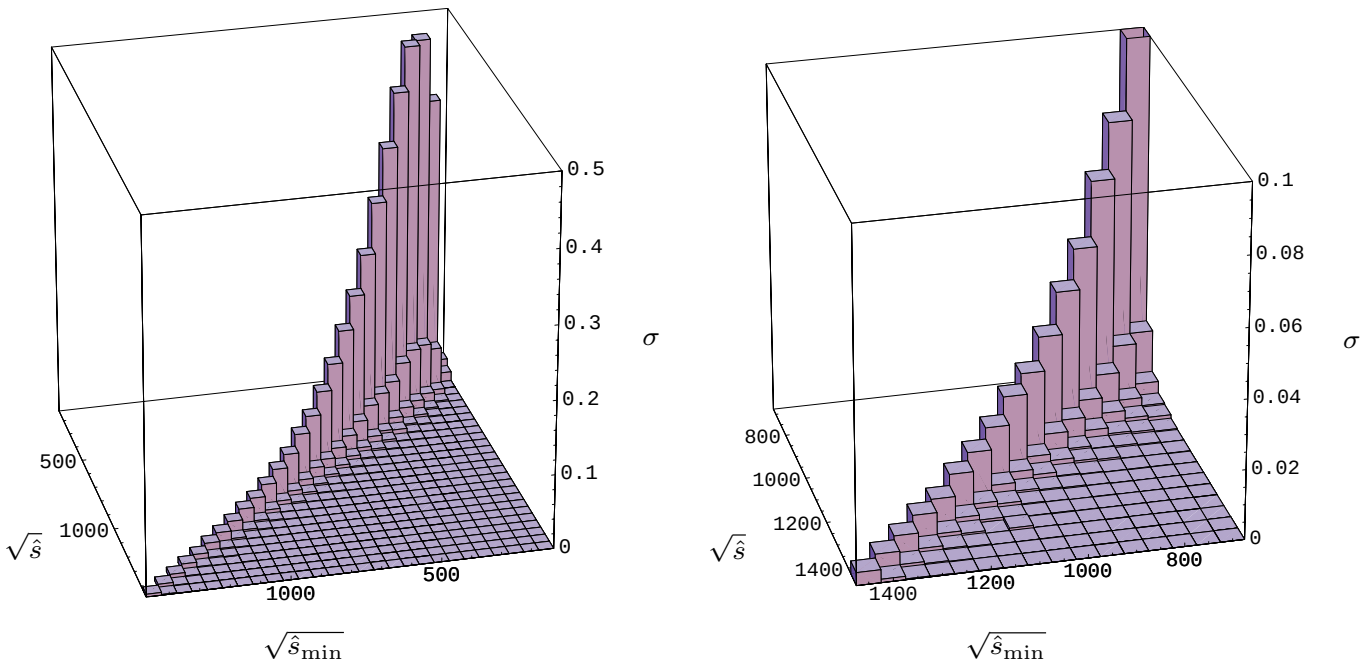

Fig. 7. The same as Fig. 6 but with huge anomalous couplings $\Delta\kappa = 0.8,\ \lambda = 0.2$ and $\Lambda = 1$ TeV

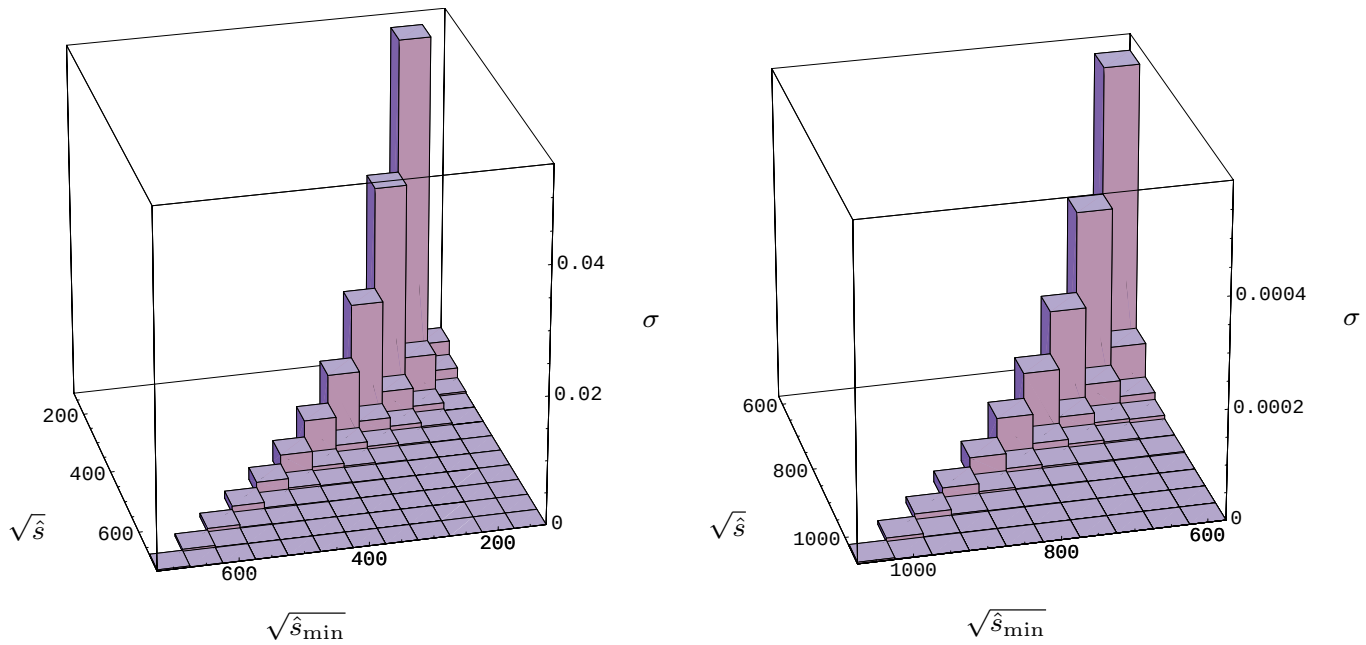

Fig. 8. The same as Fig. 6 but for Tevatron

next-to-leading order in α_s. The leptonic decay of the W and Z-boson respectively has been included in the narrow-width approximation. We retained all spin information via decay angle correlations and thereby generalized previous calculations [9–11]. We also included anomalous triple gauge boson couplings at NLO in α_s and presented the analytical expressions for the corresponding amplitudes.

As an illustration of the usefulness of the program, we have studied several observables for the LHC. Generally we find that the NLO corrections are relevant for all of them, confirming results of [8–11].

Moreover, we searched for the kinematical regions were the effect of anomalous couplings is amplified and proposed an alternative way to study its energy dependence. Using the strong correlations between the partonic center of mass energy and a measurable variable, $\hat{s}_{\min}$, makes it possible to extract anomalous couplings from the data without need to introduce ad hoc form factors. Such an

analysis is possible even for the $W\gamma$ process and, in our view, should be undertaken at the Tevatron and LHC.

Acknowledgements. It is a pleasure to thank Z. Kunszt for his participation on the initial stages of this work and for helpful discussions. D. de F. would like to thank the Department of Physics of the University of Durham for its hospitality while part of this work was carried out. This work was partly supported by the EU Fourth Framework Programme 'Training and Mobility of Researchers', Network 'Quantum Chromodynamics and the Deep Structure of Elementary Particles', contract FMRX-CT98-0194 (DG 12 - MIHT).

Appendix

The helicity amplitudes that are needed for the calculation of $W\gamma$ and $Z\gamma$ production at next-to-leading order can be found in [12]. In this appendix we list the additional amplitudes that are needed in the presence of anomalous couplings which lead to the non-standard vertices as given in (3) and (4). We use the notation and conventions of [12, 20].

We start with the $W\gamma$ amplitudes. In order to maintain electromagnetic gauge invariance we set $g_1^\gamma = 0$ and only allow anomalous couplings $\Delta\kappa^\gamma$ and λ^γ. The only diagram that gets modified by these anomalous couplings is the diagram with a $WW\gamma$ coupling. Fortunately, this diagram does not contribute to the rather complicated finite pieces F_γ^a, F_γ^b of the amplitudes, given in (4.6) and (4.7) of [12]. Therefore, only the tree-level amplitudes have to be computed with anomalous couplings.

We do not have to list the explicit results for all possible helicities of the photon and the gluon. In order to reverse the helicities of all gauge bosons, i.e. the photon and the gluon (if the latter is present), we merely have to apply a 'flip' operation, defined as

$$\text{flip2} : 1 \leftrightarrow 2;\ 3 \leftrightarrow 4;\ \langle ab\rangle \leftrightarrow [ab]\,;\ \text{and}\ A^a \leftrightarrow A^b\,(\text{for}\,W\gamma) \tag{6}$$

The amplitudes $A_\gamma^{\text{tree,a}}, A_\gamma^{\text{tree,b}}$ given in (4.4) and (4.5) of [12] are modified as follows in the presence of anomalous couplings:

$$A_{\text{AC},\gamma}^{\text{tree,a}} = A_\gamma^{\text{tree,a}} + A_{\text{AC}}^5 \tag{7}$$

$$A_{\text{AC},\gamma}^{\text{tree,b}} = A_\gamma^{\text{tree,b}} - A_{\text{AC}}^5 \tag{8}$$

where

$$A_{\text{AC}}^5 = \frac{-i\,[45]}{2s_{34}(s_{12}-s_{34})\,[34]} \times\Big((\Delta\kappa^\gamma+\lambda^\gamma)\,\langle 13\rangle\,[25]\,[34] + \lambda^\gamma\langle 1|5|2\rangle\,[45]\Big) \tag{9}$$

As usual, this will also lead to a modification of the one-loop amplitudes. The corresponding divergent pieces now read $c_\Gamma V A_{\text{AC},\gamma}^{\text{tree,a}}$ and $c_\Gamma V A_{\text{AC},\gamma}^{\text{tree,b}}$ respectively, where

$$V = -\frac{1}{\epsilon^2}\left(\frac{\mu^2}{-s_{12}}\right)^\epsilon - \frac{3}{2\epsilon}\left(\frac{\mu^2}{-s_{12}}\right)^\epsilon - \frac{7}{2}\,. \tag{10}$$

In the case of the bremsstrahlung amplitudes we have to consider two cases. The additional gluon can have positive or negative helicity. The corresponding Standard Model amplitudes are given in (4.9) to (4.12) of [12]. In the presence of anomalous couplings $\Delta\kappa$ and λ they are modified as follows.

$$A_{\text{AC},6,\gamma}^{\text{tree,a}}(1^-,2^+,3^-,4^+,5^+,6^+) = A_{6,\gamma}^{\text{tree,a}}(1^-,2^+,3^-,4^+,5^+,6^+) + A_{\text{AC}}^{6+} \tag{11}$$

$$A_{\text{AC},6,\gamma}^{\text{tree,a}}(1^-,2^+,3^-,4^+,5^-,6^+) = A_{6,\gamma}^{\text{tree,a}}(1^-,2^+,3^-,4^+,5^-,6^+) + A_{\text{AC}}^{6-} \tag{12}$$

$$A_{\text{AC},6,\gamma}^{\text{tree,b}}(1^-,2^+,3^-,4^+,5^+,6^+) = A_{6,\gamma}^{\text{tree,b}}(1^-,2^+,3^-,4^+,5^+,6^+) - A_{\text{AC}}^{6+} \tag{13}$$

$$A_{\text{AC},6,\gamma}^{\text{tree,b}}(1^-,2^+,3^-,4^+,5^-,6^+) = A_{6,\gamma}^{\text{tree,b}}(1^-,2^+,3^-,4^+,5^-,6^+) - A_{\text{AC}}^{6-} \tag{14}$$

where we defined

$$A_{\text{AC}}^{6+} \equiv i\frac{[45]\,\langle 1|2+6|5\rangle}{2\,s_{34}^2(t_{126}-s_{34})\,\langle 16\rangle\,\langle 62\rangle} \times\Big(\lambda^\gamma\,\langle 34\rangle\,\langle 15\rangle\,\langle 45\rangle + (\Delta\kappa^\gamma+\lambda^\gamma)\,\langle 13\rangle\,s_{34}\Big) \tag{15}$$

$$A_{\text{AC}}^{6-} \equiv i\frac{\langle 35\rangle\,\langle 15\rangle}{2\,s_{34}^2(t_{126}-s_{34})\,\langle 16\rangle\,\langle 62\rangle}\Big(\lambda^\gamma\,\langle 35\rangle\,\langle 1|2+6|5\rangle\,[34] -(\Delta\kappa^\gamma+\lambda^\gamma)\langle 1|2+6|4\rangle s_{34}\Big) \tag{16}$$

We now turn to the amplitudes for $Z\gamma$ production. In the Standard Model, there are no diagrams with a triple gauge boson coupling and the corresponding amplitudes $A_\gamma^{\text{tree,s}}$ can simply be obtained as the symmetric combination of the $W\gamma$ amplitudes

$$A_\gamma^{\text{tree,s}} = A_\gamma^{\text{tree,a}} + A_\gamma^{\text{tree,b}} \tag{17}$$

(see (4.15) of [12]). These combinations can be simplified somewhat but we refrain from listing the simplified versions.

The amplitudes related to an anomalous $ZZ\gamma$ or $Z\gamma\gamma$ coupling will be denoted by $A_{5/6,\text{AC}}^{(Z\gamma)}$. In the former case, the intermediate vector boson is a Z-boson whereas in the latter case it is a γ. This results in different couplings of the intermediate vector boson to the initial state quarks. Apart from this difference, the amplitudes with an intermediate Z and γ are the same. The anomalous couplings always appear in the combination

$$\tilde h_1^{Z/\gamma} \equiv \frac{h_1^{Z/\gamma}}{M_Z^2};\quad \tilde h_2^{Z/\gamma} \equiv \frac{h_2^{Z/\gamma}}{M_Z^4};\quad \tilde h_3^{Z/\gamma} \equiv \frac{h_3^{Z/\gamma}}{M_Z^2};\quad \tilde h_4^{Z/\gamma} \equiv \frac{h_4^{Z/\gamma}}{M_Z^4}. \tag{18}$$

We start with the tree-level amplitude for a positive helicity photon

$$A_{5,\text{AC}}^{(Z\gamma)} = \frac{i}{4s_{34}}\Big((i\tilde h_1^{Z/\gamma}+\tilde h_3^{Z/\gamma})2\,\langle 13\rangle\,[25]\,[45] +(i\tilde h_2^{Z/\gamma}+\tilde h_4^{Z/\gamma})\,\langle 12\rangle\,\langle 3|5|4\rangle\,[25]^2\Big) \tag{19}$$

In order to obtain the amplitudes for a negative helicity photon we have to apply the 'flip2' operation defined in (6) in addition to

$$\tilde{h}_1^{Z/\gamma} \to -\tilde{h}_1^{Z/\gamma};\ \tilde{h}_2^{Z/\gamma} \to -\tilde{h}_2^{Z/\gamma}; \tag{20}$$

The anomalous bremsstrahlung amplitude with an additional positive helicity gluon reads

$$\begin{aligned} A_{6,\mathrm{AC}}^{(Z\gamma)} = & \frac{i}{4 s_{34} \langle 16\rangle \langle 26\rangle} \\ & \times \Big((i\tilde{h}_1^{Z/\gamma} + \tilde{h}_3^{Z/\gamma}) 2 \langle 13\rangle [45] \langle 1|2+6|5\rangle \\ & + (i\tilde{h}_2^{Z/\gamma} + \tilde{h}_4^{Z/\gamma}) \langle 3|5|4\rangle \langle 1|2+6|5\rangle^2 \Big) \end{aligned} \tag{21}$$

whereas for a negative helicity gluon

$$\begin{aligned} A_{6,\mathrm{AC}}^{(Z\gamma)} = & \frac{i}{4 s_{34} [16] [26]} \\ & \times \Big((i\tilde{h}_1^{Z/\gamma} + \tilde{h}_3^{Z/\gamma}) 2 [45] [25] \langle 3|1+6|2\rangle \\ & + (i\tilde{h}_2^{Z/\gamma} + \tilde{h}_4^{Z/\gamma}) t_{126} \langle 3|5|4\rangle [25]^2 \Big) \end{aligned} \tag{22}$$

Again, the operation 'flip2' reverses the helicities of the photon and the gluon. Finally we mention that in order to get the amplitudes with a positive helicity lepton, 3^+, we simply have to exchange $3 \leftrightarrow 4$ in the amplitudes presented above. Correspondingly, the amplitudes with opposite helicities for the partons are obtained by a simple $1 \leftrightarrow 2$ crossing.

References

1. R.W. Brown, K.O. Mikaelian, Phys. Rev.D **19** (1979) 922; R.W. Brown, K.O. Mikaelian, D. Sahdev, Phys. Rev.D **20** (1979) 1164; K.O. Mikaelian, M.A. Samuel, D. Sahdev, Phys. Rev. Lett.**43** (1979) 746
2. F. Renard, Nucl. Phys.B **196** (1982) 93
3. CDF Collaboration, Phys. Rev. Lett.**74** (1995) 1936; D0 Collaboration, Phys. Rev. Lett.**75** (1995) 1034; D0 Collaboration, Phys. Rev. Lett.**78** (1997) 3634
4. CDF Collaboration, Phys. Rev. Lett.**74** (1995) 1941; D0 Collaboration, Phys. Rev. Lett.**78** (1997) 3640; D0 Collaboration, Phys. Rev.D **57** (1998) 3817
5. ALEPH Collaboration, CERN-EP/98-178, [hep-ex/9901030]; DELPHI Collaboration, Phys. Lett.B **459** (1999) 382; L3 Collaboration, Phys. Lett.B **467** (1999) 171, [hep-ex/9910008]; OPAL Collaboration, Eur. Phys. J.C **8** (1999) 191 [hep-ex/9811028]
6. H.T. Diehl (for the CDF and D0 Collaborations) in Proceedings of Vancouver 1998, vol. 1 p.520, [hep-ex/9810006]
7. J. Smith, D. Thomas, W.L. van Neerven, Z. Phys.C **44** (1989) 267
8. J. Ohnemus, Phys. Rev.D **47** (1993) 940
9. U. Baur, T. Han, J. Ohnemus, Phys. Rev.D **48** (1993) 5140 [hep-ph/9305314]
10. J. Ohnemus, Phys. Rev.D **51** (1995) 1068 [hep-ph/9407370]
11. U. Baur, T. Han, J. Ohnemus, Phys. Rev.D **57** (1998) 2823 [hep-ph/9710416]
12. L. Dixon, Z. Kunszt, A. Signer, Nucl. Phys.B **531** (1998) 3 [hep-ph/9803250]
13. J.M. Campbell, R.K. Ellis, Phys. Rev.D **60** (1999) 113006
14. S. Frixione, Z. Kunszt, A. Signer, Nucl. Phys.B **467** (1996) 399 [hep-ph/9512328]
15. G.J. Gounaris, J. Layssac, F.M. Renard, [hep-ph/9910395]
16. A.D. Martin, R.G. Roberts, W.J. Stirling, R.S. Thorne [hep-ph/9907231]
17. M. Glück, E. Reya, A. Vogt, Phys. Rev.D **48** (1993) 116, err D **51** (1995) 1427
18. S. Dittmaier, M. Bohm, A. Denner, Nucl. Phys.B **376** (1992) 29, err. B **391** (1993) 483
19. W. Beenakker et al., in Physics at LEP2, eds. G. Altarelli, T. Sjöstrand, F. Zwirner (Geneva, 1996), [hep-ph/9602351]
20. L. Dixon, Z. Kunszt, A. Signer, Phys. Rev.D **60** (1999) 114037 [hep-ph/9907305]
21. S. Frixione, Phys. Lett.B **429** (1998) 369
22. K. Hagiwara, R.D. Peccei, D. Zeppenfeld, K. Hikasa, Nucl. Phys.B **282** (1987) 253
23. M. Dobbs, Contribution to the Proceedings of the Standard Model Physics at the LHC Workshop, CERN 1999
24. D0 Collaboration, FERMILAB-PUB-99-364-E, [hep-ex/9912033]
25. U. Baur, S. Errede, G. Landsberg, Phys. Rev.D **50** (1994) 1917
26. D. Benjamin for CDF and D0 collaborations, FERMILAB-CONF-95/241-E
27. P.J. Dervan, A. Signer, W.J. Stirling, A. Werthenbach, Contribution to the Proceedings of the UK Phenomenology Workshop, Durham 1999, to be published in J. Phys. G